第 34 卷第 6 期
2018 年 6 月

无 机 化 学 学 报
CHINESE JOURNAL OF INORGANIC CHEMISTRY

Vol.34 No.6
1159-1165

两个包含联苯三羧酸配体的铜(Ⅱ)和锰(Ⅱ)配合物的合成、晶体结构及磁性质

黎 彧[1] 邹训重[1] 顾金忠*,[2] 成晓玲*,[3]

([1]广东轻工职业技术学院生态环境技术学院,
佛山市特种功能性建筑材料及其绿色制备技术工程中心,广州 510300)

([2]兰州大学化学化工学院,兰州 730000)

([3]广东工业大学轻工化工学院,广州 510006)

摘要:采用水热方法,用联苯三羧酸配体(H_3dppa)和 4,4′-联吡啶(4,4′-bipy)分别与 $CuCl_2\cdot 2H_2O$ 和 $MnCl_2\cdot 4H_2O$ 反应,合成了一个具有零维双核铜结构的配合物$[Cu_2(Hdppa)_2(4,4'\text{-bipy})(H_2O)_4]\cdot 4,4'\text{-bipy}\cdot 6H_2O$ (**1**)和一个基于双螺旋链单元的三维配位聚合物$\{[Mn_3(\mu_5\text{-dppa})_2(4,4'\text{-bipy})(H_2O)_2]\cdot 4H_2O\}_n$ (**2**),并对其结构和磁性质进行了研究。结构分析结果表明 2 个配合物分别属于三斜和单斜晶系,$P\bar{1}$ 和 $C2/c$ 空间群。配合物 **1** 具有零维双核铜结构,而且这些双核铜单元通过 O–H…O/N 氢键作用进一步形成了三维超分子框架。而配合物 **2** 中存在一个双螺旋锰链单元,这些锰链单元又通过配体进一步连接成了三维结构。研究表明,配合物 **2** 中相邻锰离子间存在反铁磁相互作用。

关键词:配位聚合物;氢键;三羧酸配体;磁性

中图分类号:O614.121;O614.71+1 **文献标识码**:A **文章编号**:1001-4861(2018)06-1159-07

DOI:10.11862/CJIC.2018.142

Syntheses, Crystal Structures and Magnetic Properties of Two Copper(Ⅱ) and Manganese(Ⅱ) Coordination Compounds Constructed from Biphenyl Tricarboxylic Acid

LI Yu[1] ZOU Xun-Zhong[1] GU Jin-Zhong*,[2] CHENG Xiao-Ling*,[3]

([1]*School of Eco-Environmental Engineering, Foshan Research Center for Special Functional Building Materials and Its Green Preparation Technology, Guangdong Industry Polytechnic, Guangzhou* 510300, *China*)

([2]*College of Chemistry and Chemical Engineering, Lanzhou University, Lanzhou* 730000, *China*)

([3]*School of Chemical Engineering and Light Industry, Guangdong University of Technology, Guangzhou* 510006, *China*)

Abstract: Zero dimensional dinuclear copper(Ⅱ) coordination compound and 3D manganese(Ⅱ) coordination polymer, namely $[Cu_2(Hdppa)_2(4,4'\text{-bipy})(H_2O)_4]\cdot 4,4'\text{-bipy}\cdot 6H_2O$ (**1**) and $\{[Mn_3(\mu_5\text{-dppa})_2(4,4'\text{-bipy})(H_2O)_2]\cdot 4H_2O\}_n$ (**2**), have been constructed hydrothermally using H_3dppa, 4,4′-bipy (H_3dppa=5-(3,4-dicarboxylphenyl)picolinic acid, 4,4′-bipy=4,4′-bipyridine), and copper or manganese chlorides. Single-crystal X-ray diffraction analyses revealed that two compounds crystallize in the triclinic or monoclinic system, space group $P\bar{1}$ or $C2/c$. In compound **1**, one 4,4′-bipy ligand bridges neighboring Cu(Ⅱ) ions to form a discrete dinuclear copper(Ⅱ) structure. These Cu_2 units are assembled to a 3D supramolecular framework through O–H…O/N hydrogen bond. In compound **2**, neighboring Mn(Ⅱ) ions are bridged by the carboxylate groups of μ_5-dppa^{3-} ligands, producing a double-helix Mn(Ⅱ) chain subunit.

收稿日期:2018-01-02。收修改稿日期:2018-03-24。

广东省高等职业院校珠江学者岗位计划资助项目(2015),广东省自然科学基金(No.2016A030313761),广东轻院珠江学者人才类项目(No.RC2015-001),生物无机与合成化学教育部重点实验室开放基金(2016),广东省高校创新团队项目(No.2017GKCXTD001)国家自然科学基金(No.21701032)和佛山市科技计划项目(No.2017AB003922)资助。

*通信联系人。E-mail:gujzh@lzu.edu.cn,ggcxl@163.com;会员登记号:S06N5892M1004(顾金忠)。

The adjacent double-helix chains subunits are further linked by the $dppa^{3-}$ blocks and 4,4′-bipy ligands into a 3D framework. Magnetic studies for compound **2** demonstrate an antiferromagnetic coupling between the adjacent Mn (Ⅱ) centers. CCDC: 1814154, **1**; 1814155, **2**.

Keywords: coordination polymer; hydrogen bonding; tricarboxylic acid; magnetic properties

0 Introduction

In recent years, the rational design and construction of coordination polymers have received remarkable attention due to their potential applications, architectures, and topologies[1-5]. There are many factors, such as the coordination geometry of the metal centers, type and connectivity of organic ligands, stoichiometry, reaction conditions, template effect, presence of auxiliary ligands, and pH values influencing the structures of target coordination polymers during self-assembly[6-10]. Among these factors, organic ligands play a noteworthy role in constructing coordination compounds.

Multi-carboxylate biphenyl ligands have been certified to be of great significance as constructors due to their strong coordination abilities in various modes, which could satisfy different geometric requirements of metal centers[8-9,11-14]. In order to extend our research in this field, we chose one biphenyl tricarboxylic acid ligand, 5-(3,4-dicarboxylphenyl)picolinic acid (H_3dppa), to construct novel coordination compounds. The ligand possesses the following features: (1) it contains a pyridyl and a phenyl ring with structural flexibility and conformation. Rotation of the C-C single bond between pyridyl and phenyl rings could form numbers of coordination geometries of metal ions. (2) It has seven potential coordination sites, one N atom from pyridyl ring and six O atoms of three carboxylate groups, which is benifical to contruct coordination polymerw with interesting structures by its rich coordination modes. (3) It can act as hydrogen-bond acceptor as well as donor, depending upon the degree of deprotonation.

Taking into account these factors, we herein report the syntheses, crystal structures and magnetic properties of two Cu (Ⅱ) and Mn (Ⅱ) coordination compounds constructed from biphenyl tricarboxylic acid ligands.

1 Experimental

1.1 Reagents and physical measurement

All chemicals and solvents were of AR grade and used without further purification. Carbon, hydrogen and nitrogen were determined using an Elementar Vario EL elemental analyzer. IR spectra were recorded using KBr pellets and a Bruker EQUINOX 55 spectrometer. Thermogravimetric analysis (TGA) data were collected on a LINSEIS STA PT1600 thermal analyzer with a heating rate of 10 ℃·min^{-1}. Magnetic susceptibility data were collected in the 2 ~300 K temperature range with a Quantum Design SQUID Magnetometer MPMS XL-7 with a field of 0.1 T. A correction was made for the diamagnetic contribution prior to data analysis.

1.2 Synthesis of $[Cu_2(Hdppa)_2(4,4'\text{-bipy})(H_2O)_4]\cdot 4,4'\text{-bipy}\cdot 6H_2O$ (1)

A mixture of $CuCl_2\cdot 2H_2O$ (0.051 g, 0.30 mmol), H_3dppa (0.086 g, 0.30 mmol), 4,4′-bipy (0.047 g, 0.3 mmol), NaOH (0.024 g, 0.60 mmol), and H_2O (10 mL) was stirred at room temperature for 15 min, and then sealed in a 25 mL Teflon-lined stainless steel vessel, and heated at 160 ℃ for 3 days, followed by cooling to room temperature at a rate of 10 ℃·h^{-1}. Blue block-shaped crystals of **1** were isolated manually, and washed with distilled water. Yield: 55% (based on H_3dppa). Anal. Calcd. for $C_{48}H_{50}Cu_2N_6O_{22}$(%): C 48.44, H 4.23, N 7.06; Found (%): C 48.59, H 4.27, N 7.02. IR (KBr, cm^{-1}): 3 667w, 3 317w, 2 979w, 1 726w, 1 603s, 1 557w, 1 493w, 1 423w, 1 382s, 1 347s, 1 307w, 1 254 m, 1 225w, 1 143w, 1 073w, 1 044w, 892w, 852w, 828w, 805m, 700w, 664w, 642w, 583w.

1.3 Synthesis of $\{[Mn_3(\mu_5\text{-dppa})_2(4,4'\text{-bipy})(H_2O)_2]\cdot 4H_2O\}_n$ (2)

The synthesis of **2** was similar as compound **1**

using $MnCl_2 \cdot 4H_2O$ (0.059 g, 0.30 mmol) instead of $CuCl_2 \cdot 2H_2O$. Yellow block-shaped crystals of **2** were gained. Yield: 60% (based on H_3dppa). Anal. Calcd. for $C_{38}H_{32}Mn_3N_4O_{18}$(%): C 45.76, H 3.23, N 5.62; Found (%): C 45.61, H 3.21, N 5.65. IR (KBr, cm^{-1}): 3 504w, 3 312w, 2 921w, 1 592s, 1 562s, 1 487w, 1 428w, 1 399 m, 1 307w, 1 248w, 1 213w, 1 160w, 1 090w, 1 062w, 1 026w, 1 003w, 921w, 903w, 852m, 811m, 706w, 658w, 630w, 589w. The compounds are insoluble in water and common organic solvents, such as methanol, ethanol, acetone and DMF.

1.4 Structure determinations

The diffraction data of two single crystals with dimensions of 0.25 mm×0.23 mm×0.21 mm (**1**) and 0.28 mm×0.23 mm×0.21 mm (**2**) was collected at 293(2) K on a Bruker SMART APEX Ⅱ CCD diffractometer with Mo $K\alpha$ radiation (λ=0.071 073 nm). The structures were solved by direct methods and refined by full matrix least-square on F^2 using the SHELXTL-2014 program[15]. All non-hydrogen atoms were refined anisotropically. All the hydrogen atoms were positioned geometrically and refined using a riding model. A summary of the crystallography data and structure refinements for **1** and **2** is given in Table 1. The selected bond lengths and angles for compounds **1** and **2** are listed in Table 2. Hydrogen bond parameters of compounds **1** and **2** are given in Table 3.

CCDC: 1814154, **1**; 1814155, **2**.

Table 1　Crystal data for compounds 1 and 2

Compound	1	2
Chemical formula	$C_{48}H_{50}Cu_2N_6O_{22}$	$C_{38}H_{32}Mn_3N_4O_{18}$
Molecular weight	1 190.02	997.49
Crystal system	Triclinic	Monoclinic
Space group	$P\bar{1}$	$C2/c$
a / nm	0.710 81(6)	2.481 35(10)
b / nm	0.940 17(5)	0.736 26(3)
c / nm	1.843 62(10)	2.400 42(9)
α / (°)	90.217(4)	
β / (°)	96.594(6)	115.444(5)
γ / (°)	99.334(6)	
V / nm^3	1.207 38(14)	3.960 0(3)
Z	1	4
F(000)	614	2 028
Crystal size / mm	0.25×0.23×0.22	0.28×0.23×0.21
θ range for data collection	3.338~25.049	3.244~25.049
Limiting indices	$-8 \leqslant h \leqslant 8, -11 \leqslant k \leqslant 10, -20 \leqslant l \leqslant 21$	$-29 \leqslant h \leqslant 29, -8 \leqslant k \leqslant 8, -28 \leqslant l \leqslant 24$
Reflection collected, unique (R_{int})	7 727, 4 274 (0.036 5)	7 289, 3 518 (0.038 8)
D_c / ($g \cdot cm^{-3}$)	1.637	1.673
μ / mm^{-1}	0.975	1.028
Data, restraint, parameter	4 274, 0, 355	3 518, 0, 297
Goodness-of-fit on F^2	1.026	1.053
Final R indices [$I \geqslant 2\sigma(I)$] R_1, wR_2	0.055 8, 0.127 8	0.046 1, 0.100 4
R indices (all data) R_1, wR_2	0.075 0, 0.143 1	0.064 8, 0.113 3
Largest diff. peak and hole / ($e \cdot nm^{-3}$)	943 and −1 029	518 and −490

Table 2　Selected bond distances (nm) and bond angles (°) for compounds 1 and 2

1					
Cu(1)-O(2)	0.196 7(3)	Cu(1)-O(7)	0.222 3(3)	Cu(1)-O(8)	0.197 5(3)
Cu(1)-N(1)	0.199 4(3)	Cu(1)-N(2)	0.199 9(3)		

Continued Table 2

O(2)-Cu(1)-O(8)	161.32(13)	O(2)-Cu(1)-N(1)	82.37(13)	O(8)-Cu(1)-N(1)	96.55(13)
O(2)-Cu(1)-N(2)	87.90(14)	O(8)-Cu(1)-N(2)	91.46(14)	N(1)-Cu(1)-N(2)	169.57(15)
O(2)-Cu(1)-O(7)	105.19(13)	O(8)-Cu(1)-O(7)	93.49(13)	N(1)-Cu(1)-O(7)	93.56(13)
N(2)-Cu(1)-O(7)	92.61(13)				
			2		
Mn(1)-O(1)	0.218 6(3)	Mn(1)-O(1)A	0.218 6(3)	Mn(1)-O(4)B	0.214 2(2)
Mn(1)-O(4)C	0.214 2(2)	Mn(1)-O(7)	0.222 7(2)	Mn(1)-O(7)A	0.222 7(2)
Mn(2)-O(2)	0.221 0(2)	Mn(2)-O(3)	0.215 3(2)	Mn(2)-O(5)D	0.216 5(2)
Mn(2)-O(6)E	0.214 9(3)	Mn(2)-N(1)D	0.230 2(3)	Mn(2)-N(2)	0.226 6(3)
O(4)B-Mn(1)-O(4)C	96.63(14)	O(4)B-Mn(1)-O(1)	87.90(10)	O(4)C-Mn(1)-O(1)	170.61(9)
O(1)-Mn(1)-O(1)A	88.84(15)	O(4)B-Mn(1)-O(7)A	85.31(9)	O(4)C-Mn(1)-O(7)A	94.25(9)
O(1)-Mn(1)-O(7)A	94.32(9)	O(1)-Mn(1)-O(7)	86.15(9)	O(7)-Mn(1)-O(7)A	179.35(14)
O(6)E-Mn(2)-O(3)	85.37(10)	O(6)E-Mn(2)-O(5)D	96.99(10)	O(3)-Mn(2)-O(5)D	176.51(10)
O(6)E-Mn(2)-O(2)	170.00(9)	O(3)-Mn(2)-O(2)	84.78(9)	O(5)D-Mn(2)-O(2)	92.77(10)
O(6)E-Mn(2)-N(2)	87.30(11)	O(3)-Mn(2)-N(2)	90.95(10)	O(5)D-Mn(2)-N(2)	86.61(10)
O(2)-Mn(2)-N(2)	91.11(10)	O(6)E-Mn(2)-N(1)D	92.09(10)	O(3)-Mn(2)-N(1)D	108.60(9)
O(5)D-Mn(2)-N(1)D	73.95(9)	O(2)-Mn(2)-N(1)D	92.71(10)	N(2)-Mn(2)-N(1)D	160.34(10)

Symmetry codes: A: $-x$, y, $-z+1/2$; B: x, $y+1$, z; C: $-x$, $y+1$, $-z+1/2$; D: $-x+1/2$, $-y+1/2$, $-z+1$; E: x, $-y$, $z-1/2$ for **2**.

Table 3 Hydrogen bond parameters of compounds 1 and 2

D–H···A	*d*(D-H) / nm	*d*(H···A) / nm	*d*(D···A) / nm	∠DHA / (°)
		1		
O(5)–H(1)···N(4)A	0.082	0.183	0.260 3	157.6
O(7)–H(1W)···O(1)B	0.085	0.187	0.272 3	179.6
O(7)–H(2W)···O(11)C	0.073	0.199	0.271 5	171.6
O(8)–H(3W)···O(4)D	0.085	0.184	0.268 8	179.5
O(8)–H(4W)···O(5)A	0.085	0.175	0.260 3	179.5
O(9)–H(5W)···O(10)E	0.085	0.188	0.273 3	179.3
O(9)–H(6W)···O(3)A	0.085	0.184	0.268 5	178.2
O(10)–H(7W)···O(4)D	0.085	0.194	0.278 8	178.3
O(11)–H(9W)···O3)A	0.085	0.189	0.274 4	179.0
O(11)–H(10W)···O(4)D	0.085	0.216	0.300 9	179.2
		2		
O(7)–H(1W)···O(3)A	0.086	0.224	0.294 4	138.8
O(8)–H(3W)···O(2)B	0.085	0.213	0.293 6	159.0

Symmetry codes: A: $-x+1$, $-y+1$, $-z+1$; B: $x-1$, y, z; C: x, $y-1$, z; D: $-x+2$, $-y+1$, $-z+1$; E: $-x+1$, $-y+1$, $-z$ for **1**; A: x, $y+1$, z; B: $-x+1/2$, $y-1/2$, $-z+1/2$ for **2**.

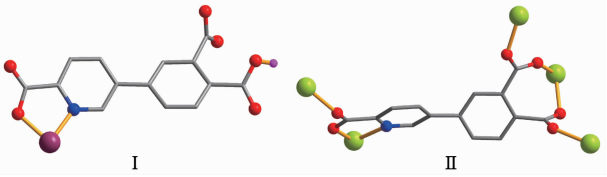
2 Results and discussion

2.1 Description of the structure

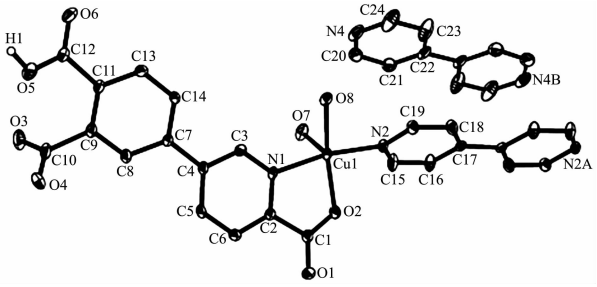
2.1.1 $[Cu_2(Hdppa)_2(4,4'\text{-bipy})(H_2O)_4]\cdot 4,4'\text{-bipy}\cdot 6H_2O$ (**1**)

Single-crystal X-ray diffraction analysis reveals that compound **1** crystallizes in the triclinic space group $P\bar{1}$. Its asymmetric unit contains one crystallographically unique Cu(Ⅱ) atom, one $Hdppa^{2-}$ block, a half of one 4,4′-bipy moiety, two H_2O ligands, a half of one free 4,4′-bipy ligand, and three lattice water molecules. As depicted in Fig.1, Cu1 atom is surrounded by three O and two N atoms in a slightly distorted $\{CuO_3N_2\}$ square-pyramidal geometry

with the τ value of 0.138 (τ=0 for a regular square-pyramidal geometry and τ=1 for a perfect trigonal-bipyramidal geometry)[16]. The two O (O2 and O8) and two N (N1 and N2) atoms occupy the basal plane, and one O (O7) atom resides at the apical position of the coordination polyhedron. The lengths of the Cu-O bonds range from 0.196 7(3) to 0.222 3(3) nm, whereas the Cu-N distances vary from 0.199 4(3) to 0.199 9(3) nm; these bonding parameters are comparable to those found in other reported Cu(Ⅱ) compounds[14,17]. In **1**, the $Hdppa^{2-}$ ligand adopts terminal coordination mode (mode Ⅰ, Scheme 1), in which the deprotonated carboxylate groups show the monodentate or uncoordinated modes. The dihedral angle between pyridyl and phenyl rings in the $Hdppa^{2-}$ is 17.51°. Two crystallographically equal Cu(Ⅱ) centers are bridged by the 4,4′-bipy ligand to form a discrete dinuclear copper(Ⅱ) structure with a Cu…Cu separation of 1.104(3) nm (Fig.2). These Cu_2 units are assembled to a 3D supramolecular framework through O–H…O/N hydrogen bond (Fig.3 and Table 3).



Scheme 1　Coordination modes of $Hdppa^{2-}$ / $dppa^{3-}$ ligands in compounds **1** and **2**

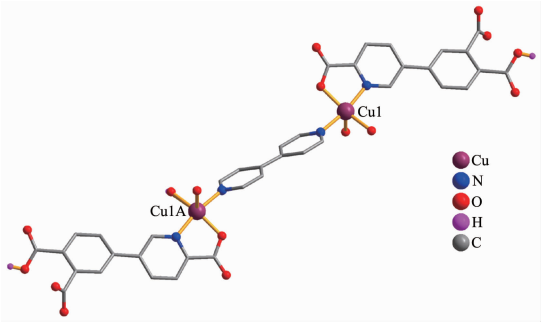


H atoms and lattice water molecules were omitted for clarity except the H atom of COOH group; Symmetry codes: A: –*x*+1, –*y*, –*z*; B: –*x*+2, –*y*, –*z*

Fig.1　Drawing of the asymmetric unit of compound **1** with 30% probability thermal ellipsoids

2.1.2　$\{[Mn_3(\mu_5\text{-dppa})_2(4,4'\text{-bipy})(H_2O)_2]\cdot 4H_2O\}_n$ (**2**)

The asymmetric unit of **2** consists of two crystallographically distinct Mn atoms (Mn1 with half occupancy; Mn2 with full occupancy), one μ_5-$appa^{3-}$ block, a half of one 4,4′-bipy ligand, one coordinated and two lattice water molecules. As shown in Fig.4, six-coordinate Mn1 atom reveals a distorted octahedral $\{MnO_6\}$ environment, filled by four carboxylate O atoms from four individual μ_5-$dppa^{3-}$ blocks and two O atoms from two H_2O ligands. The Mn2 center is coordinated by four carboxylate O atoms from three distinct $dppa^{3-}$ moieties and two N atoms from two different 4,4′-bipy ligands, thus composing octahedral $\{MnO_4N_2\}$ geometry. The Mn-O distances range from 0.214 2(2) to 0.222 7(2) nm, whereas the Mn-N



H atoms are omitted for clarity except the H atoms of the COOH groups; Symmetry codes: A: –*x*+1, –*y*, –*z*

Fig.2　Dinuclear Cu(Ⅱ) unit of **1**

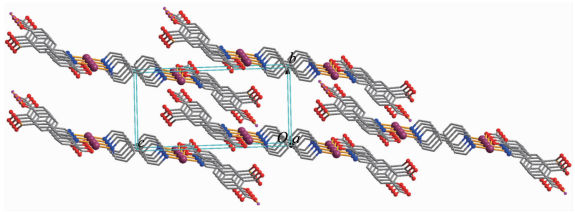
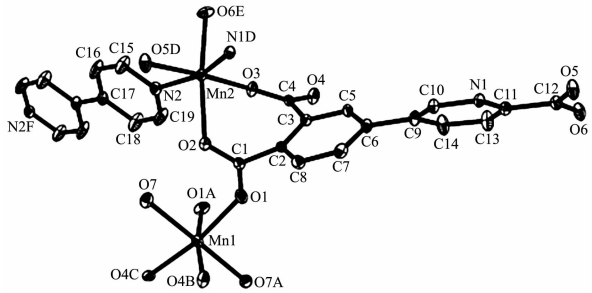


Fig.3　Perspective of 3D supramolecular framework parallel to the *bc* plane in **1**



H atoms were omitted for clarity; Symmetry codes: A: –*x*, *y*, –*z*+1/2; B: *x*, *y*+1, *z*; C: –*x*, *y*+1, –*z*+1/2; D: –*x*+1/2, –*y*+1/2, –*z*+1; E: *x*, –*y*, *z*–1/2; F: –*x*, –*y*+1, –*z*

Fig.4　Drawing of the asymmetric unit of compound **2** with 30% probability thermal ellipsoids

distances vary from 0.226 6(3) to 0.230 2(3) nm; these bonding parameters are comparable to those observed in other Mn(Ⅱ) compounds[9,11,13]. In **2**, the $dppa^{3-}$ block acts as a μ_5-N,O_6-spacer and its COO^- groups take a bidentate bridging mode (mode Ⅱ, Scheme 1). In $dppa^{3-}$, a dihedral angle (between pyridyl and benzene rings) is 46.31°. The carboxylate groups of $dppa^{3-}$ blocks bridge alternately neighboring Mn atoms to form the infinite right-handed or left-handed helical Mn-O-C-O-Mn chains (Fig.5) with the Mn…Mn separation of 0.545 7(2) and 0.534 8(2) nm. Two types of these helical chains are interconnected to each other through the Mn(Ⅱ) centers to produce a double-helix chain (Fig.5). The adjacent double-helix subunits are further linked by the $cptc^{3-}$ blocks into a 2D sheet (Fig.6). These 2D sheets are arranged into a 3D framework by further coordination interactions of the $dppa^{3-}$ and 4,4′-bipy ligands to Mn atoms (Fig.7).

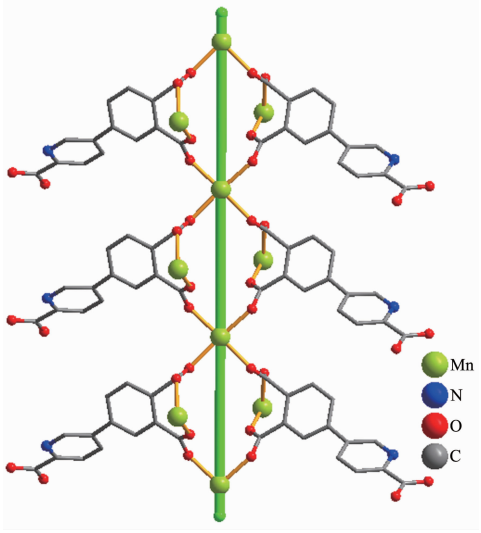


Fig.5 Double-helix chain unit in compound **2**

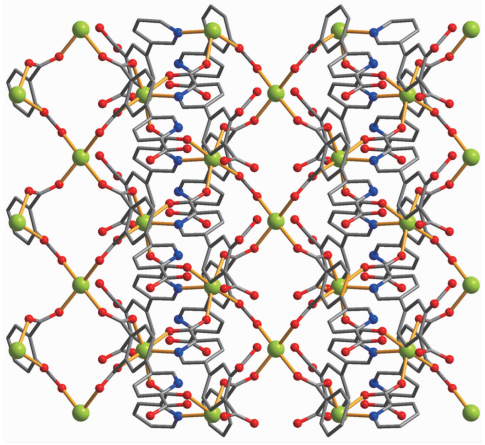


Fig.6 Two dimensional sheet along the *c* axis in compound **2**

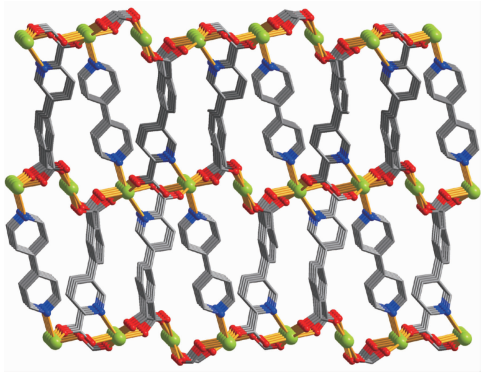


Fig.7 Three dimensional framework along the *b* axis in compound **2**

2.2 TGA analysis

To determine the thermal stability of compounds **1** and **2**, their thermal behaviors were investigated under nitrogen atmosphere by thermogravimetric analysis (TGA). As shown in Fig.8, compound **1** loses its six lattice water molecules in the range of 41~162 ℃ (Obsd. 8.8%, Calcd. 9.1%), followed by the decomposition at 218 ℃. The TGA curve of **2** reveals that four lattice and two coordinated water molecules are released between 78 and 230 ℃ (Obsd. 10.5%, Calcd. 10.8%), and the dehydrated solid begins to decompose at 334 ℃.

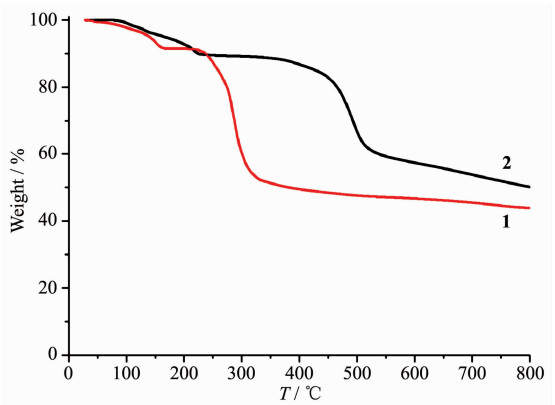


Fig.8 TGA curves of compounds **1** and **2**

2.3 Magnetic properties

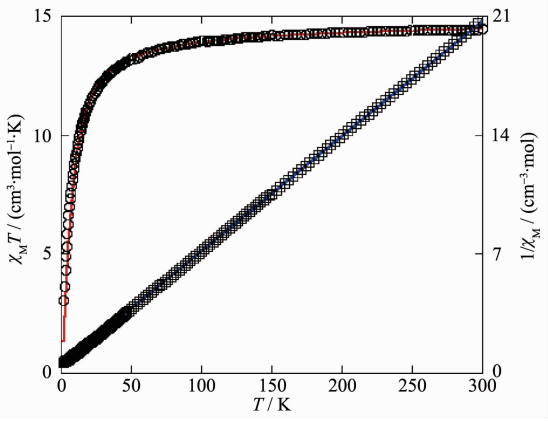
Variable-temperature magnetic susceptibility studies were carried out on powder sample of **2** in the 2~300 K temperature range. The $\chi_M T$ value at 300 K is 14.48 $cm^3 \cdot mol^{-1} \cdot K$, which is larger than the value of 13.12 $cm^3 \cdot mol^{-1} \cdot K$ expected for three magnetically

isolated high-spin Mn(Ⅱ) centers (S_{Mn}=5/2, g=2.0). Upon cooling, the $\chi_M T$ value drops down very slowly from 14.48 $cm^3 \cdot mol^{-1} \cdot K$ at 300 K to 13.97 $cm^3 \cdot mol^{-1} \cdot K$ at 100 K and then decreases steeply to 3.04 $cm^3 \cdot mol^{-1} \cdot K$ at 2 K (Fig.9). The χ_M^{-1} vs T plot for **2** in the 2~300 K range obeys the Curie-Weiss law with a Weiss constant θ of −6.88 K and a Curie constant C of 14.78 $cm^3 \cdot mol^{-1} \cdot K$. The negative value of θ and the decrease of the $\chi_M T$ should be attributed to the overall antiferromagnetic coupling between the Mn(Ⅱ) centers within double-helix chain unit. We attempted to fit the data for **2** by applying the following expression[18] for a 1D Mn(Ⅱ) chain:

$$H=-JS_iS_j$$

$$\chi_{chain}=[Ng^2\beta^2/(kT)](A+Bx^2)(1+Cx+Dx^3)^{-1}$$

with A=2.916 7, B=208.04, C=15.543, D=2 707.2, and $x=|J|/(kT)$.



Solid curve represents the best fit to the equations in the text and the line shows the Curie-Weiss fitting

Fig.9　Temperature dependence of $\chi_M T$ (○) and $1/\chi_M$(□) vs T for compound **2**

The susceptibility for **2** was simulated using this rough model, and resulting in J=−3.01 cm^{-1}, g=2.07, and $R=4.98\times10^{-5}$. The negative J parameter indicates a weak antiferromagnetic exchange coupling between the adjacent Mn(Ⅱ) centers in **2**, which is in agreement with a negative θ value.

3　Conclusions

In summary, two new coordination compounds, namely $[Cu_2(Hdppa)_2(4,4'\text{-bipy})(H_2O)_4]\cdot 4,4'\text{-bipy}\cdot 6H_2O$ (**1**) and $\{[Mn_3(\mu_5\text{-dppa})_2(4,4'\text{-bipy})(H_2O)_2]\cdot 4H_2O\}_n$ (**2**), have been synthesized under hydrothermal conditions. The compounds feature the 0D dinuclear and 3D framework structures, respectively. Magnetic studies show an antiferromagnetic coupling between the adjacent Mn(Ⅱ) centers in **2**.

References:

[1] Hu Z G, Zhao D. *CrystEngComm*, **2017**,**19**:4066-4081

[2] Lv R, Li H, Su J, et al. *Inorg. Chem.*, **2017**,**56**:12348-12356

[3] Li P Z, Wang X J, Liu J, et al. *CrystEngComm*, **2017**,**19**:4157-4161

[4] Cui Y, Yue Y, Qian G, et al. *Chem. Rev.*, **2012**,**112**:1126-1162

[5] Kuppler R J, Timmons D J, Fang Q R, et al. *Coord. Chem. Rev.*, **2009**,**253**:3042-3066

[6] Gu J Z, Cui Y H, Liang X X, et al. *Cryst. Growth Des.*, **2016**,**16**:4658-4670

[7] Ji P F, Manna K, Lin Z, et al. *J. Am. Chem. Soc.*, **2016**,**138**:12234-12242

[8] Gu J Z, Gao Z Q, Tang Y. *Cryst. Growth Des.*, **2012**,**12**:3312-3323

[9] Gu J Z, Wu J, Lv D Y, et al. *Dalton Trans.*, **2013**,**42**:4822-4830

[10]Du M, Li C P, Liu C S, et al. *Coord. Chem. Rev.*, **2013**,**257**:1282-1305

[11]Gu J Z, Liang X X, Cui Y H, et al. *CrystEngComm*, **2017**,**19**:117-128

[12]LU Ya(鲁雅), LÜ Tian-Xi(吕天喜), HU Wei-Ji(胡未极), et al. *Chinese J. Inorg. Chem.*(无机化学学报), **2017**,**33**(10):1869-1875

[13]ZHAO Su-Qin(赵素琴), GU Jin-Zhong(顾金忠). *Chinese J. Inorg. Chem.*(无机化学学报), **2016**,**32**(9):1611-1618

[14]CHEN Jin-Wei(陈金伟), WEN Bing-Song(温炳松), CAO Fang-Li(曹芳利), et al. *Chinese J. Inorg. Chem.*(无机化学学报), **2017**,**33**(12):2322-2328

[15]Spek A L. *Acta Crystallogr. Sect. C: Struct. Chem.*, **2015**,**C71**:9-18

[16]Addison A W, Rao T N, Reedijk J, et al. *J. Chem. Soc. Dalton Trans.*, **1984**:1349-1356

[17]Gu J Z, Liang X X, Cai Y, et al. *Dalton Trans.*, **2017**,**46**:10908-10925

[18]Hiller W, Strhel J, Datz A, et al. *J. Am. Chem. Soc.*, **1984**,**106**:329-335